KERNFORSCHUNGSZENTRUM

KARLSRUHE

Sensitivity Studies for Fast Reactor Whole Core Accidents

R. Fröhlich, P. Schmuck, D. Thiem
(Gesellschaft für Kernforschung mbH)

G. Evrard, A. Renard, M. Stievenart
(Fa. Belgonucléaire, Brüssel)

GESELLSCHAFT FÜR KERNFORSCHUNG M. B. H.
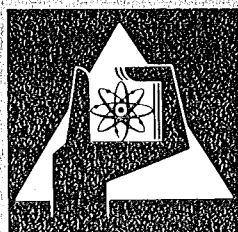
KARLSRUHE

KERNFORSCHUNGSZENTRUM KARLSRUHE

KFK 2086

Institut für Neutronenphysik und Reaktortechnik
Projekt Schneller Brüter

Sensitivity Studies for Fast Reactor Whole

Core Accidents

by

G. Evrard[1], R. Fröhlich[2], A. Renard[1],

P. Schmuck[2], M. Stievenart[1], D. Thiem[2]

1 Firma Belgonucleaire, Brüssel

2 Institut für Neutronenphysik u. Reaktortechnik,
   Gesellschaft für Kernforschung, Karlsruhe

Abstract

The energy yield of a hypothetical transient overpower accident of an
LMFBR is strongly influenced by core design parameters. The sensitivity
of this type of accident on some interesting design parameters is studied
for the fresh SNR 300 Mark 1 core. In addition the sensitivity of the
energy yield on other parameters of more speculative nature, e.g. the
fuel coolant interaction parameters and the pin failure location, is
analysed. The codes CARMEN 2 and KADIS are used for the analyses of the
predisassembly and disassembly phases respectively. Most of the parameter
variations are performed consistently for the predisassembly and the
disassembly phases. Areas are indicated where further experimental and
theoretical work is needed.

Sensitivitätsstudien für einen schweren, hypothetischen Leistungsstörfall
eines schnellen, natriumgekühlten Brüters

Zusammenfassung

Die Energieausbeute eines hypothetischen Leistungsstörfalls bei einem
schnellen, natriumgekühlten Brüter wird stark von den core Entwurfs-
parametern beeinflußt. Die Sensitivität dieses Unfalltyps auf Änderungen
gewisser Entwurfsparameter wird anhand des SNR 300 Mark 1 cores untersucht.
Der Einfluß anderer Parameter von mehr spekulativer Natur, wie z.B. der
Brennstoff-Natrium-Reaktions-Parameter oder die Stelle des Pinversagens,
wird ebenfalls studiert. Die Programme CARMEN 2 und KADIS werden für die
Berechnung der Predisassembly- respektive der Disassembly-Phase verwendet.
Fast alle Parametervariationen werden in der Predisassembly- und der
Disassembly-Phase konsistent durchgeführt. Zum Schluß wird auf einige Punkte
hingewiesen, die weitere experimentelle bzw. theoretische Arbeiten erfordern.

Table of contents

1. Introduction

For the SNR-300 reactor, two hypothetical whole core accidents are important:

1. Insertion of reactivity (e.g. by a certain ramp rate) with simultaneous failure of both shut-down systems.

2. A primary coolant pump failure (flow coastdown) with simultaneous failure of both shut-down systems.

An unlimited reactivity insertion of 5 $/sec was chosen to represent the class of reactivity accidents. The study presented here investigates only this accident. It should be mentioned that some studies performed by Heusener, Kessler and Lauber at the Argonne National Laboratory /1/, have shown that this 5 $/sec ramp accident gives a higher energy release than the loss of coolant accident.

The calculations concern the so-called Mark-1 fresh core of the SNR-300 reactor with half inserted control rods.

The accident calculations start with nominal steady state conditions. Then one observes for this reactivity accident, the following sequence of events: increase of power and of material temperatures, pin failure, fuel-coolant interaction, core voiding with the associated increase of reactivity. In case of a sufficient pressure build-up, which can cause material displacements, one enters into the so-called disassembly phase of calculation. In the process of core disassembling the fuel is dispersed and this mechanism leads to a first nuclear shut down of the system.

In contrast to other sensitivity studies which vary the parameters in the disassembly phase only /2/, the sensitivity studies presented here are consistently done, i.e. parameter variations in the pre-disassembly and in the disassembly phase are performed in a consistent manner.

The predisassembly phase of the calculations is performed by the CARMEN-2 code /3/, developed by BELGONUCLEAIRE while the disassembly phase is

calculated by the KADIS code developed by INR/GfK. For all calculations the computer facilities of the GfK in Karlsruhe were used.

The data transfer between CARMEN and KADIS is initiated by a switch-over criterion based upon the average temperature in the hottest fuel pellet of the core.

For this sensitivity study, we varied several important parameters of the CARMEN/KADIS input data, for instance, the radial power distribution, the average power per pin, the velocity of sodium expulsion, the inserted reactivity ramp rate, the values of the Doppler coefficients, the distribution of the sodium density and of the sodium void reactivity, and the location of the fuel pin failure.

2. Description of the predisassembly code CARMEN-2

2.1. Calculation method:

This code was developed to calculate the dynamic behaviour of a sodium cooled fast reactor in accidental conditions, especially those which can imply local coolant boiling and core voiding. It can handle typical reactivity accidents such as control rod ejection or start-up accidents, it can also take into account flow rate perturbations such as pump failure or local blockages, and third it can consider variations of inlet coolant temperature and of outlet pressure.

The CARMEN-2 code utilizes point neutron kinetics with space dependent feedbacks, multiregion heat transfer in cylindrical geometry with temperature dependent properties, monitoring of fuel pin failure, coolant boiling and ejection out of the channels. The reactivity feedbacks associated with the various physical phenomena involved in the pre-disassembly phase are taken into account. The Doppler is different when a channel is filled with coolant or voided from it. The voiding scheme is precalculated by a fuel-coolant interaction model in an independent code, and is specified by input data in CARMEN. For the calculations presented in this paper, the sodium voiding is assumed to start with a

delay time of 4 milliseconds after pin failure, the velocities of sodium expulsion are almost constant.

2.2. Geometrical model of the SNR-300-Mark-1 core

The geometrical model considers a reactor core with two radial zones of different fuel enrichment. The core is divided radially in concentric rings, each represented by an average channel, which can accomodate independent features and different input flow conditions. The total number of characteristic channels is limited presently to nine. For these studies, there are six channels in the first radial core zone, three in the second one (see figure 1). Each channel is represented by one typical fuel pin, its cladding and the associated coolant. The structural material of a fuel subassembly is simulated by an equivalent cylindrical wrapper tube.

Axially each channel is divided into several axial meshes (maximum = 17) along the core itself and the lower and upper axial blankets. The mesh dimension is uniform within each of those three axial regions but can be different from one to the other.

At each level, the materials are divided into radial concentric layers, presently, there are five layers for fuel, two for cladding, one for the bulk coolant and one for structure.

3. Results of the predisassembly calculations

3.1. Variations of the radial power distribution, of the average power per fuel pin, of the sodium voiding velocity, of the input ramp rate.

The base problem and four independent variations of it are summarized in table I.

The parameter variations are non-cumulative. They are respectively:

1) In case 2, a flatter radial power distribution (see figure 2) is considered, which gives a radial power shape factor equal to 1.169 (case 2) instead of 1.368 (base case).

2) In case 3, a 20 % reduction of the average power by fuel pin is assumed.

3) In case 4, a reduction of the voiding velocity of sodium due to fuel-coolant interaction is studied: the voiding velocity of the base case is divided by 3.

4) In case 5, a lower reactivity ramp, i.e. a 50 ¢/sec ramp rate, is used.

For each case, the results (ramp, reactivity, power, energy) are given at the beginning of disassembly, that is at the time of transfer to the KADIS code. The threshold temperature for the switch over criterion is the average temperature of $3250^{o}C$ in the hottest pellet. The positive reactivity ramp transferred from predisassembly to disassembly calculations takes into account all the reactivity components, except the Doppler effect. The total reactivity and the power for the switch over time are also transferred to KADIS.

1) With the flatter power distribution, the core disassembly happens later and more channels are involved in the voiding process; the ramp increases by 35 %, the total reactivity by 2 %, the power level by 34 % and the energy stored in the fuel by 22 %.

2) The reduction of the average power per pin delays the start of disassembly, but the number of failed channels is the same as in the base case and the main results are much less influenced than in the preceding case.

3) The reduction of the voiding velocity (as indicated in some recent
publications, (e.g. /4/) which corresponds to a softer fuel-coolant
interaction reduces drastically the ramp (-55 %), the total reactivity
(-5.5 %) and the final power (-50 %).

4) In the last case of this table, one can see that with the lower
ramp, the delay between first pin failure and disassembly start is
much longer (65 ms for this case, 13 ms for the base case); due to
this fact, the core regions voided from sodium are much bigger than
in the base case; the sodium void in this case extends up to the core
regions where it has a negative effect; the balance between positive
and negative sodium effect gives a decrease of the transferred reactivity
ramp and of the total reactivity.

The figure 3 shows the time evolution of the reactor power for case 1
(base case), 2 (with flatter radial power distribution) and 4 (with
reduced core voiding velocity). The times of fuel pin failure initiation
are indicated for each channel (channel 1 is at the core centre; channel 7
is the hottest one of the second zone of enrichment). Before the first
pin failure, the Doppler feedback moderates the power increase; then, core
voiding induces a positive reactivity effect.

The figure 4 gives the evolution of the positive reactivity ramp just
before the start of disassembly. The arrows correspond to the voiding
initiation time in the various channels, which occurs 4 milliseconds after
pin failure. One can see that each successive core channel voiding increases
stepwise the reactivity ramp.

On figure 5, one can see the evolution of the different components of
the reactivity, for the base case, just before the beginning of disassembly.
A remarkable feature is the maximum of the total reactivity. This follows
from an increase due to the sodium void reactivity, and from a decrease
due to the Doppler feedback. When we transfer the data to this disassembly
code, we are very close to this maximum. Switching to the disassembly phase
for the maximum value of the reactivity appears to be a pessimistic assumption.

3.2 Variation of the sodium reactivity distribution

Figure 6 shows the sodium density distributions which were used for
the sensitivity study. The picture gives the radial distribution of the
value per cubic centimeter of the sodium density coefficient in a radial
traverse which is located just below core midplane.

The curve N1 is the nominal distribution, which is used in the base case.
For the curve N2, one has taken a shape similar to the nominal one, but
the total positive value of the Na density reactivity is increased by a
factor of 55 %.

The value of 55 % was chosen because we intended to compare two different
reactor designs for the SNR-300 core, that is the more recent SNR Mark-1A
design with the older Mark-1 design. The Mark-1A core has a higher fuel
inventory, a flatter power distribution, and higher sodium void and density
reactivity values. For the Mark-1A core the absolute value of the total
positive sodium density reactivity is 55 % higher than for the Mark-1 core.
The F curve is a flatter distribution, similar to the distribution of the
Mark-1A core; with this curve, we have also a 55 % increase of the total
positive sodium reactivity, but the shape is typical of a large core.

On Table II, one can see the effects of the changes of Na reactivity
distribution. Case 1 is the base case. In case 6, we take the sodium
density reactivity distribution N2 which has the same shape but with an
increase of 55 % for the positive value. For what concerns the Na void
reactivity distribution, the distribution has the same shape as the Na
density reactivity distribution, but the increase of the positive value
is only 28 %. This value of 28 % originates also from the comparison study
with the other design (Mark-1A) of the SNR reactor.

In case 7, the increases of Na void and density reactivity are the same
as in case 6, but the shape of both distributions is flatter (curve F
of figure 6).

For case 8, we take the flatter curve but we increase the both reactivities
(density and void)by 55 percent.

The results show an increase of the positive ramp, with a big effect between the base case 1 and case 6, approximately the same values for cases 6 and 7, and with an increase between case 7 and 8.

There is also an increase, which is more progressive, for the total reactivity. It was checked that the value of the transferred total reactivity is very important for the disassembly phase. We can see also how the effects of the total sodium void reactivity and of the shape of the sodium reactivity distribution differ with respect to their importance.

We can also notice increases of the power and of the stored energy, but this is less important for the energy release during the disassembly phase.

3.3 Variation of the Doppler coefficients:

Figure 7 shows the results of the sensitivity studies on the Doppler feedback reactivity. In each case, the Doppler coefficients for each channel were multiplied by a constant factor.

The times of core disassembly beginning and of first pin failure and the total reactivity transferred to KADIS are plotted as functions of the multiplicating factor of the Doppler coefficients. When the absolute value of the negative Doppler increases, one can observe the following effects:

1) the disassembly occurs later
2) the time interval between first pin failure and start of disassembly becomes larger.
3) there is a decrease of the total reactivity at the end of the pre-disassembly phase. But it decreases by a smaller factor than the increase of the Doppler, because there is also an increase of the possitive reactivity due to the inserted reactivity ramp (due to 1), and an increase of the sodium void reactivity because the duration of voiding is larger (due to 2).

3.4 Variation of the location of pin failure and variation of the reactivity insertion ramp

On figure 8, we have displayed the results of the sensitivity study for a variation of the pin failure location.

The remarkable feature is that the assumed fuel-coolant interaction process gives a maximum reactivity effect for a failure location below the midplane. This effect can be explained by the dimensions and the location of the sodium voids at the transfer to KADIS. These voids are shown on figure 9:the sodium void is represented at the beginning of disassembly for 3 cases of different pin failure: the base case (pin failure is about 5 cm below core midplane), pin failure 14 cm below and 14 cm above core midplane. The maximum void occurs when the pin failure is located 14 cm below core midplane. This is mainly due to the different velocities of the upper and lower void boundaries. For the case where the failure is located 14 cm above core midplane, there is also a big void, but it is extended to regions where the sodium voiding gives a less positive effect and even to regions where it gives a negative effect.

Figure 9 shows also the case with the lower ramp rate of 50 cents per second. As it is written in section 3.1, this case gives a very important sodium voiding but the total void reactivity is not so big because the void is extended to regions with a negative effect in the core and in the upper axial blanket.

4. Description of the disassembly code KADIS

4.1 Physical and computational models

First we give a short presentation of the models used in the disassembly code KADIS /5/. KADIS evolved from an early version of the ANL's VENUS program /6/.

Coupled fluid dynamic and neutronic equations are solved in R-Z-Geometry. A finite difference scheme in space and time is used to solve the 2-D-hydrodynamic equations of an isotropic, non viscous fluid in Lagrangian coordinates. The neutronics is represented by space averaged (i.e. point) kinetics, which describes the time history of the fission power level. Six groups of delayed neutrons are taken into account.

During the disassembly phase the fuel is heated up adiabatically. Heat transfer from fuel to sodium is allowed only when a fuel-coolant inter-action (FCI) is specified for a mesh cell. A mesh cell is the smallest unit used in the hydrodynamics calculational procedure.
The energy content of the fuel in a mesh cell determines the pressure build-up. Two effects occur when the temperature rises:

a) the solid and liquid fuel expands and fills more and more the voids, which may exist.

b) the vapor pressure of fuel rises.

If there is little void space in a mesh cell, for instance in a reactivity accident where the core is almost full of sodium the void space will be filled by the expanding fuel in an early stage of the excursion. High one phase pressures are developed and they lead to an early and fast disassembly. The compressibility of sodium and structural steel is taken into account when calculating the one phase pressure.

If we deal with a sodium out situation - typical for a flow coast down accident - there will be much more free volume in a mesh cell and no one-phase pressures can develop. The temperatures will rise then to about 5000 degrees Kelvin to provide a vapor pressure sufficiently high for fast disassembly.

Two different reactivity feedback mechanisms are considered in our calculation:

a) Doppler feedback
b) disassembly feedback

The Doppler feedback is computed regionwise using mass averaged temperatures. The disassembly feedback – which is induced by the material movement – is calculated by first order perturbation theory.

In KADIS a fuel-coolant interaction in a mesh cell is represented by the Cho and Wright parametric model /7/. This model allows to account for the fragmentation and mixing mechanism of fuel in a rough manner in specifying a mixing time constant.

When the FCI is started in a mesh cell (it is triggered by the fuel temperature) energy is transferred to liquid sodium and the high pressure yield is mainly due to:

a) the sodium thermal expansion; this is important when a mesh cell stays in the one phase region.

b) the sodium vaporization; this is important for a mesh cell in the two phase region.

The pressure will be mainly determined by the thermo-physical properties of sodium.

The fuel-coolant interaction in the predisassembly and the disassembly phase are not calculated in a consistent manner, because it is not possible to take over the time history of the FCI from the CARMEN code. Presently a FCI calculation must be initiated in the KADIS code. Therefore we use the FCI only optionally in the KADIS code, it is not the standard for a disassembly calculation now.

It should be mentioned that the KADIS code was developed out of an earlier version of the ANL-VENUS code. The most important differences and additions are:

- a fuel-coolant interaction module (Cho & Wright model /7/);
- procedures to calculate and edit the mass, energy and temperature of molten fuel;
- simulation of purely axial material movements;
- regionwise edit of the reactivity feedback (axially and radially separated) and of the Doppler feedback;

- plotting routines for the time dependent quantities and for the
  Lagrangian mesh;
- dynamic storage allocation for a large number of one and two-
  dimensional arrays.

At the time of switchover from the predisassembly to the disassembly phase
two criteria must be fulfilled:

a) the reactor is above prompt critical

b) the (specific) thermal energy accumulated in the predisassembly phase
   is high enough; the criterion is checked by the temperatures in the
   pellets.

One point should be stressed here:

The thermal and hydrodynamic processes are described in the disassembly
phase in a more homogenized manner than in the predisassembly phase.
For instance temperatures, densities used in the disassembly code KADIS
are averaged over some pellets. Space dependent variables - for instance
the maximum temperature of the fuel shown in our tables - must therefore
always be looked at as averaged quantities.

4.2 Geometrical model of the SNR 300 Mark 1 core

In Fig. 10 the regions of the SNR 300-Mark 1 model are shown. Each region
is used in a homogenized way in the nuclear calculations which provide
as input data for KADIS the Doppler reactivity coefficients and the total
material reactivity worth curves. The total material reactivity worth
data and the Doppler reactivity data for KADIS were calculated by Heusener,
Keßler and Lauber using first order perturbation theory. A more detailed
discussion of the core model used is given in their report /1/. Regions
2, 4, 6, 9, 10, 12, 13, 15 represent the core area. The remaining regions
refer to the blanket. In the regions 4, 9 and 12 followers and in the
regions 10 and 13 control rods are accounted for in the homogenization.

Fig. 11 shows an radial traverse of the total material reactivity worth just below the midplane. For the moment the original traverse in this plot is considered. The large dips in this curve refer to the regions 4, 9 and 12, respectively, which contain follower material. In the disassembly feedback formalism only gradients of the worth curves are used. The second - artificially flattened - traverse is used in our sensitivity study.

5. Results of the disassembly calculations and Discussions

We present now the results of our sensitivity study for the disassembly phase. These results refer to cases already introduced in the description of the predisassembly phase.

In Fig. 12 a plot of the power history of the base case is given which has been computed without and with fuel coolant interaction in the disassembly phase. The mixing time constant is assumed to be 3 milliseconds for the FCI case, the particle radius 150 μ. The case without FCI can be regarded as having a mixing time constant of infinite magnitude. The high pressure build up in the FCI-case leads to an earlier nuclear shut down of the reactor. Therefore less energy can be accumulated compared to the base case. The short duration of the disassembly phase should be noted (only about 4 msec are needed for the base case). This short time gives some guarantee that the physical models of KADIS will be applicable during this ramp accident calculation.

Fig. 13 shows the reactivity contributions in the disassembly phase for the base case. First we have the ramp of 58 $/sec which rises from the initial reactivity level. The net reactivity shows a decrease during the whole disassembly phase. During the first two milliseconds only the Doppler feedback is of importance. After this time the disassembly feed-back comes in quickly and leads to nuclear shut down. The physical quantities in the following tables refer mainly to the end of disassembly, which is defined by nuclear shut down (nuclear power less then 10 000 MW).

The base case - the first column in Table III - shows the following features:

A ramp of 58 $/sec, an initial reactivity of 1.087 $ and a rather high initial power, 0.635 million Megawatt are KADIS input data. The maximum power is about doubled compared to the initial value - this was already shown in figure 12 containing the power history.
The most interesting result in this table is the energy deposited in the molten fuel. Its value in the base case is 2676 Megajoules and will be used for comparison later. The energy deposited in molten fuel reflects the destruction potential of the hypothetical accident under consideration. (By definition this amount of energy is set free when the molten fuel is cooled down to the melting temperature and solidified !). The destruction potential is also reflected in the mass of molten fuel - 4324 kg - and the average temperature of molten fuel - 3814 degree Kelvin.
The total energy release - 3260 MJ in the base case - is given here only for reference. It represents the time integrated fission power for the disassembly phase only.

The results of the second column of this table are calculated with an artificially flattened radial power distribution (this corresponds to case 2 in table I). The higher initial ramp and initial reactivity originate from a more coherent voiding process. The result is a much higher energy yield; the energy deposited in molten fuel has increased by 42 %. This value is higher than the total energy released during disassembly. This is no error in our calculation, it only demonstrates that the flatter distribution gives much more molten fuel already at switch over time.

In the third column we present results for case 3 (see table I) where the power per pin was 20 % lower than in the base case. The influence on the energy of molten fuel is rather weak; there is only an increase of 6 % compared to the base case.

The last column of this table displays case 4 (see table I) where the voiding velocity has been divided by 3 to simulate a softer FCI /4/. The energy content of molten fuel is 50 % lower compared to the base case and also the mass of molten fuel is reduced remarkably.

In the first two cases shown on table IV the fuel-coolant interaction
module of KADIS has been used starting from the base case data.
The two cases refer to two different mixing time constants:
3 milliseconds and 10 milliseconds. The duration of the disassembly is
decreased for the two cases, but more markedly for the 3 millisecond
case. For the energy deposited in molten fuel we get a 49 % decrease in
the 3 millisecond case and only a 8 % decrease in the 10 millisecond-
case compared to the base case without fuel-coolant interaction in the
disassembly phase.

The sensitivity with respect to total material reactivity worth curves
has also been studied with the KADIS program. The total material reactivity
values have been divided by 3. This means also a reduction of the
disassembly feedback by this factor. In fig. 11 a radial traverse of this
flattened worth curve has been shown. The third column in table IV shows
that we get an increase of 12 % for the energy deposited in molten fuel.

In Table V the KADIS results of the sodium reactivity sensitivity study
are displayed. The three cases have been already introduced and explained
earlier (see § 3.2). Here s.v. means sodium void reactivity, s.d. sodium
density reactivity. In the first two cases the sodium void coefficients
were changed by 28 %, the sodium density coefficients by 55 %. These
values were chosen to simulate the SNR 300 Mark 1A core. Also, a flatter
radial distribution was taken into account which corresponds to the
Mark 1a core. In the first case we get 19 % more energy deposited in
molten fuel, in the second case 27 % (compared to the base case). Because
of some doubts with respect to the accuracy of void coefficient calculations -
they are done by first order perturbation theory - the second case has
been recalculated with sodium void coefficients increased by 55 %. Here
we arrive at a 36 % energy increase.

In Table VI we show results of calculations with the pin failure criterion
changed and with a lower ramp. The first column of this table corresponds
to the case where the pin fails 14 cm above core midplane, i.e. about
at 1/4 of the distance between the midplane an the upper core boundary.
The initial reactivity and the ramp are rather low because the voiding

process reaches areas with negative reactivity contributions. The
energy of the molten fuel is decreased by 48 % against the base case.

If the pin fails 14 cm below the midplane - corresponding to the second
column in table VI - we get only a 5 % higher energy content of molten
fuel.

Another parameter of high interest is the initiating ramp of a
reactivity accident[*]. In column 3 we give the results for an accident
with an initiating ramp of 50 cents per second. It is surprising that
this low initiation ramp leads to a relatively high reactivity value
and a relatively high ramp rate at the begin of the disassembly cal-
culation (26.7 $/sec and 1.05 $). Therefore the energy of molten fuel
is only 42 % lower compared to the base case where the accident was
initiated by a 5 $/sec ramp.

In Fig. 14 we show the effect of a variation of the Doppler coefficients
on the energy deposited in molten fuel. The coefficients were multiplied
by a uniform factor. The plot shows the energy of molten fuel versus this
factor. The base case can be found when the factor is 1. In the dashed
curve FCI has been included in the disassembly phase with a mixing time
constant of 3 milliseconds. We can see that in the neighborhood of the
base case the energy is a monotonic decreasing function of the Doppler
strength.

---

[*]All cases up to now were initiated by 5 $/sec-ramps

6. Conclusions

Finally, we summarize some important items of this investigations
and try to outline some conclusions.

In almost all calculations presented in this report parameter variations
for the initiating phase and the disassembly phase have been done
consistently. The influence of the changed parameters on the accident
consequence , especially on the energy deposited in the molten fuel
at the end of the disassembly phase, has been studied in detail.

Parameter variations reflect the uncertainties of these quantities in
the following respects:

(1) For a given core design the parameters as e.g. the power distribution,
    the sodium void reactivity, the Doppler reactivity are calculated
    with a large error margin.

(2) It is of interest to change "differentially" some core design para-
    meters, to study their influence on the accident history independently.

(3) Some parameter changes, e.g. the change of the location of the pin
    failure or the variation of FCI-parameters reflect the lack of
    experimental evidence about the mechanism of these effects. The
    initiating reactivity ramp rate may well belong to this class of
    parameters.

In the class of design parameters the power distribution, the sodium
and Doppler reactivities have a strong influence on the energy deposited
in the molten fuel. There is not so strong a dependence on the total
initial power and the total material reactivity worth curves.

In the class of "unknown" parameters the pin failure location is of
high interest having a strong influence on the energy yield. More
experimental evidence for the pin failure mechanism is needed. The FCI -
not fully consistently treated in the predisassembly and the disassembly

calculation - seems also to have some potential for a decrease of the energy yield. In this case a further development of the code systems is necessary, but also further experimental work on the basic FCI-parameters is important to narrow the uncertainty margin.

Finally a remark concerning the "pessimistic" philosophy used in reactor safety considerations seems to be in order.
Usually one predetermines some "obviously" pessimistic parameters and goes through the accident calculation. As physical pictures used in the predisassembly and disassembly calculation are very different it is sometimes not possible to predict what is really pessimistic or optimistic a priori. As an example one could consider the fuel particle size used by the Cho-Wright model of the fuel coolant interaction. If the particle size is small, this will result during the predisassembly phase a high pressure building in channels and therefore a high sodium voiding ramp rate will occur. This leads to a high reactivity ramp rate as input into the disassembly calculation. There will also be high pressure buildup from the FCI in the disassembly calculation, which leads to faster material movement and to early shut down. Therefore a small particle size will lead to two competing effects which might cancel each other partially. The extent of the cancellation will be heavily influenced by other parameters (e.g. the initiating ramp rate which determine the failure time for a channel and therefore the voiding pattern of the core). As a result, one must be extremely careful with statements indicating that a parameter choice or a model assumption is pessimistic or optimistic with respect to a base case situation before one has not completed the analysis for the specific cases considered.

References

/1/   G. HEUSENER, G. KESSLER, H. LAUBER
         Analysis of Hypothetical Accidents for SNR-300;
         KFK 1834 (September 1973)

/2/ a.   R.B. NICHOLSON & J.F. JACKSON
         Analysis of Disassembly Accident, including computer code
         Development and Sensitivity Studies;
         ANL 7800 (1970)

    b.   R.A. MEYER, B. WOLFE, N.F. FRIEDMAN, R. SEIFERT
         Fast Reactor Meltdown Accidents, using Bethe-Tait Analysis;
         GEAP - 4809 (1967)

/3/   A. RENARD & R. KUNZI
         CARMEN 2. A Multichannel Computer Code for the Dynamic
         Analysis of Accidents in a Na-cooled Fast Reactor;
         BN 7310-03 (October 1973)

/4/   Analysis of Hypothetical Core Disruptive Accident (HCDA),
         April - December 1972;
         GEAP - 13921 (December 1972)

/5/   P. SCHMUCK, A. ARNECKE, R. FRÖHLICH, G. JACOBS
         Untersuchungen und Programmentwicklungen zu Disassembly-Vor-
         gängen in Natriumgekühlten Schnellen Reaktoren;
         KFK 1272/4 (1973)

/6/ a.   W.T. SHA & T.H. HUGHES
         VENUS: A Two Dimensional Coupled Neutronics-Hydrodynamics
         Computer Program for Fast Reactor Power Excursions;
         ANL 7701 (1970)

    b.   J.F. JACKSON & R.B. NICHOLSON
         VENUS II: A LMFBR Disassembly Program;
         ANL 7951 (1972)

/7/   D.H. CHO, R.O. IVINS, R. W. WRIGHT
      A Rate-Limited Model of Fuel/Coolant Interactions: Model
      Development and Preliminary Calculations ;
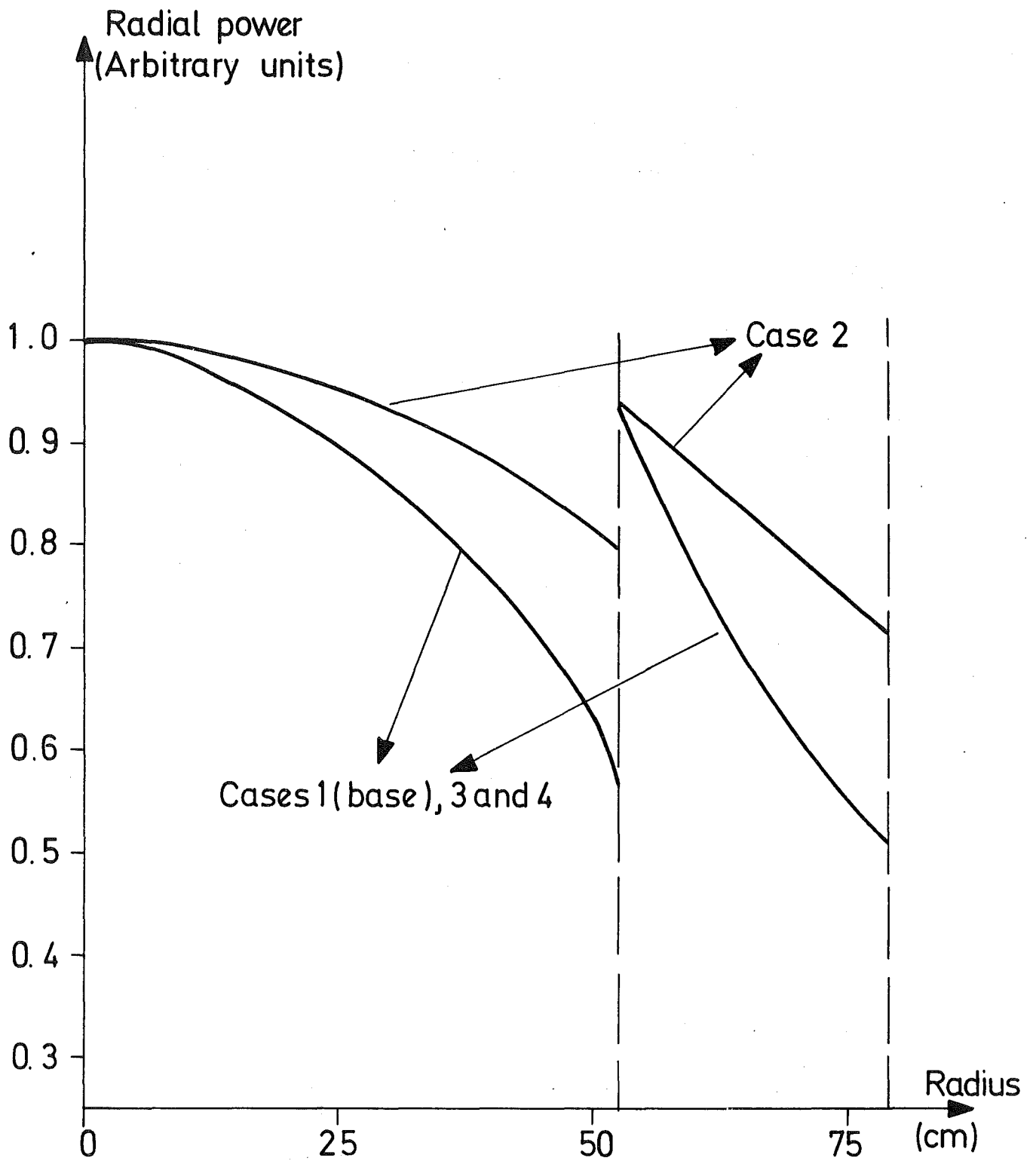   ANL 7919

Figure and Table Captions

Fig. 1 : Geometrical model of the SNR 300 Mark 1 core

Fig. 2 : Radial power distribution used in CARMEN/KADIS calculations

Fig. 3 : Normalized power during predisassembly phase

Fig. 4 : Positive Reactivity ramp rates during the predisassembly phase

Fig. 5 : Reactivity components during the predisassembly phase

Fig. 6 : Radial sodium density reactivity distribution used in CARMEN

Fig. 7 : Total reactivity, time of the first pin failure and time
of switchover to the disassembly calculation as a function
of the Doppler strength

Fig. 8 : Total reactivity and ramp as a function of the failure position

Fig. 9 : Sodium voiding pattern at the beginning of disassembly

Fig. 10: KADIS region scheme for the calculation of the reactivity
coefficients (Doppler and total material worth curves)

Fig. 11: Radial traverse of the total material worth curves

Fig. 12: Power history during the disassembly phase for the base
case without and with FCI

Fig. 13: Reactivity components during the disassembly phase for the
base case without and with FCI

Fig. 14: Energy of molten fuel as a function of the Doppler strength

Tab. I : Input data and results of CARMEN predisassembly calculations

Tab. II: Input data and results of CARMEN predisassembly calculations

Tab. III:Results of consistent CARMEN/KADIS sensitivity calculations

Tab. IV: Results of sensitivity studies with KADIS

Tab. V : Results of CARMEN/KADIS calculations with changed sodium
reactivity coefficients

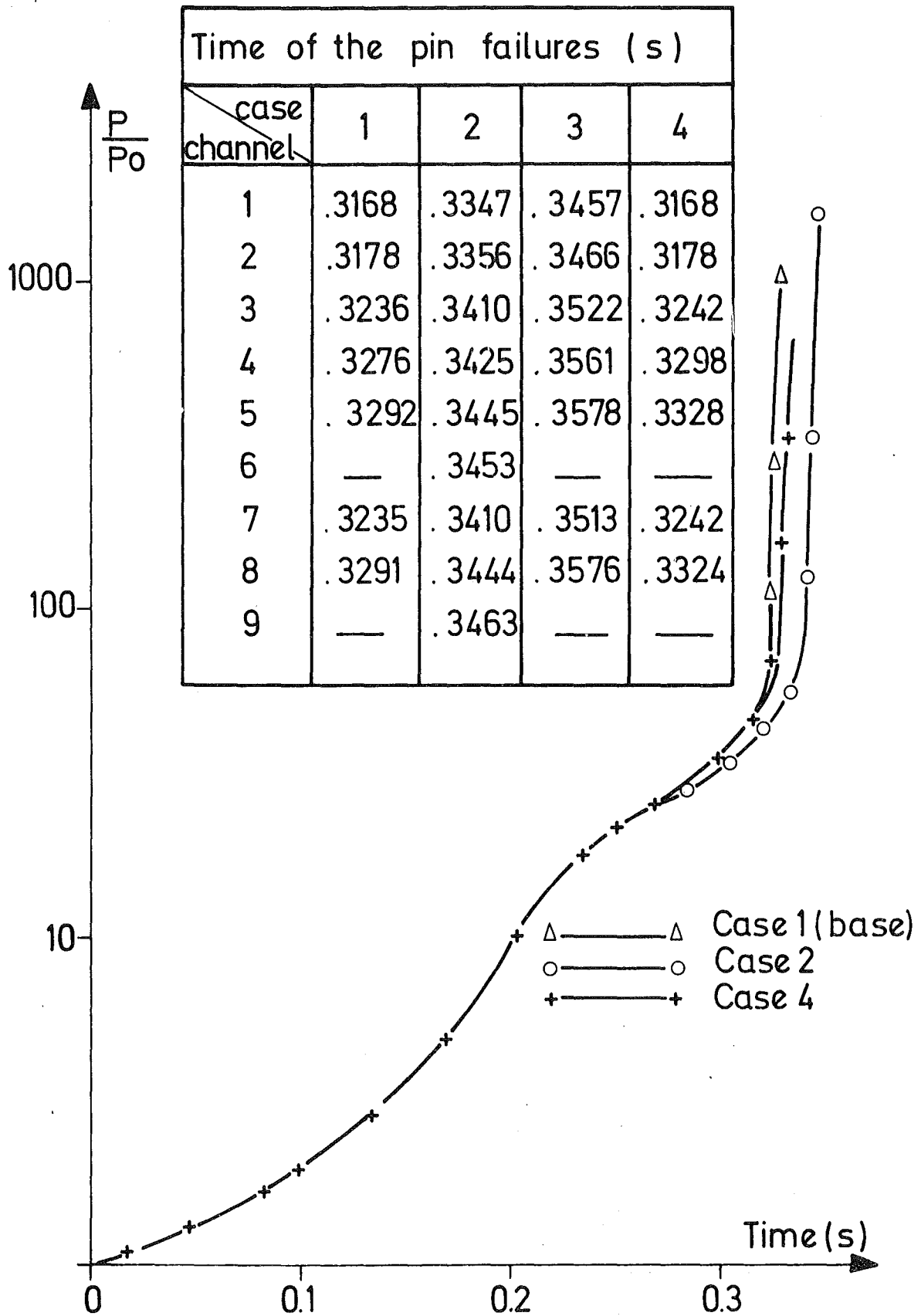Tab. VI: Results of CARMEN/KADIS calculations with changed pin failure
location and lower ramp
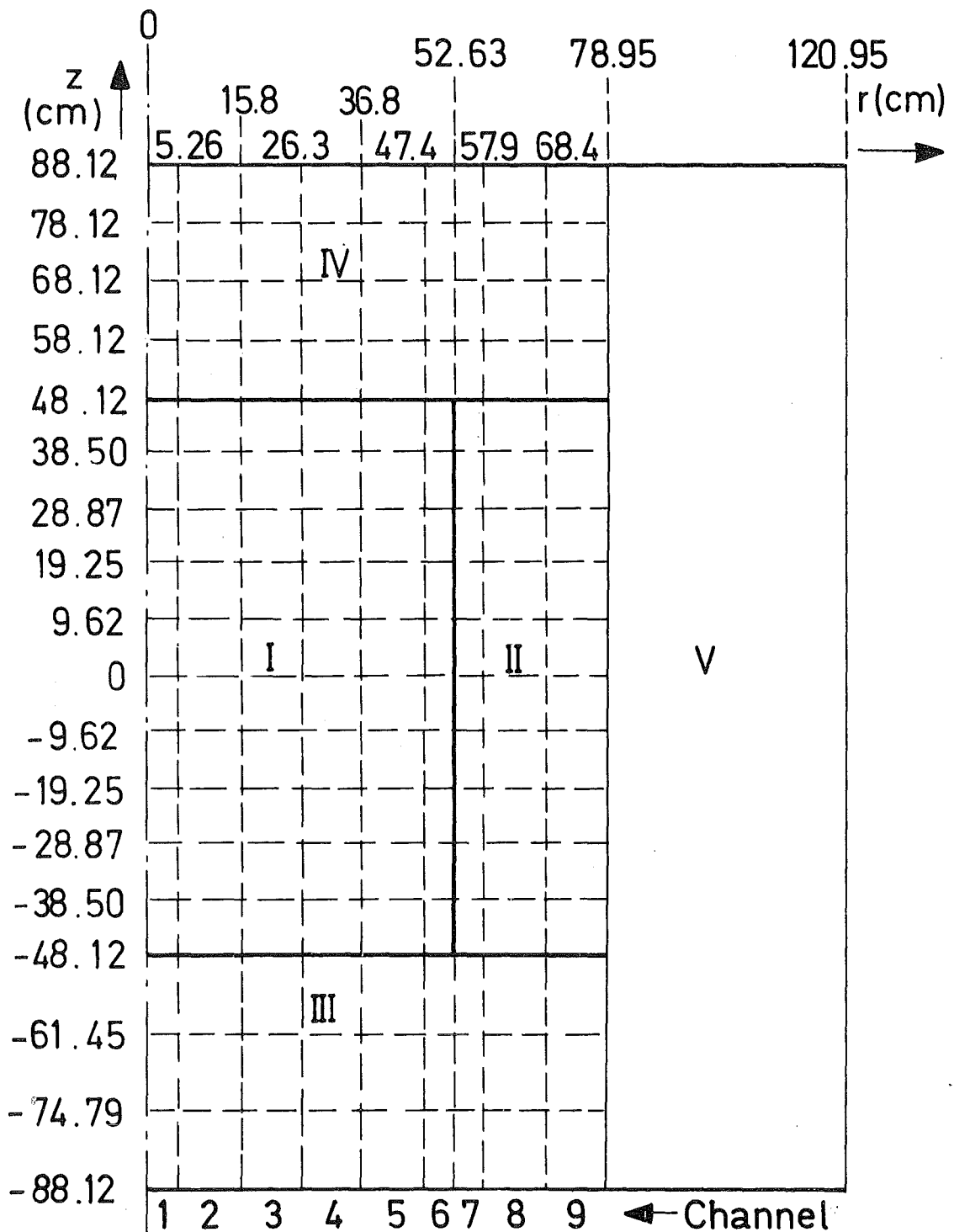
SNR 300 MARK 1 CORE GEOMETRICAL MODEL

FIG.1

I   Inner core zone   IV   Upper axial blanket
II   Outer core zone   V   Radial blanket.
III Lower axial blanket

RADIAL POWER DISTRIBUTION

FIG.2

Time of the pin failures (s)				
case ⟍ channel	1	2	3	4
1	.3168	.3347	.3457	.3168
2	.3178	.3356	.3466	.3178
3	.3236	.3410	.3522	.3242
4	.3276	.3425	.3561	.3298
5	.3292	.3445	.3578	.3328
6	—	.3453	—	—
7	.3235	.3410	.3513	.3242
8	.3291	.3444	.3576	.3324
9	—	.3463	—	—

△————△ Case 1 (base)
○————○ Case 2
+————+ Case 4

NORMALIZED POWER VERSUS TIME FIG.3
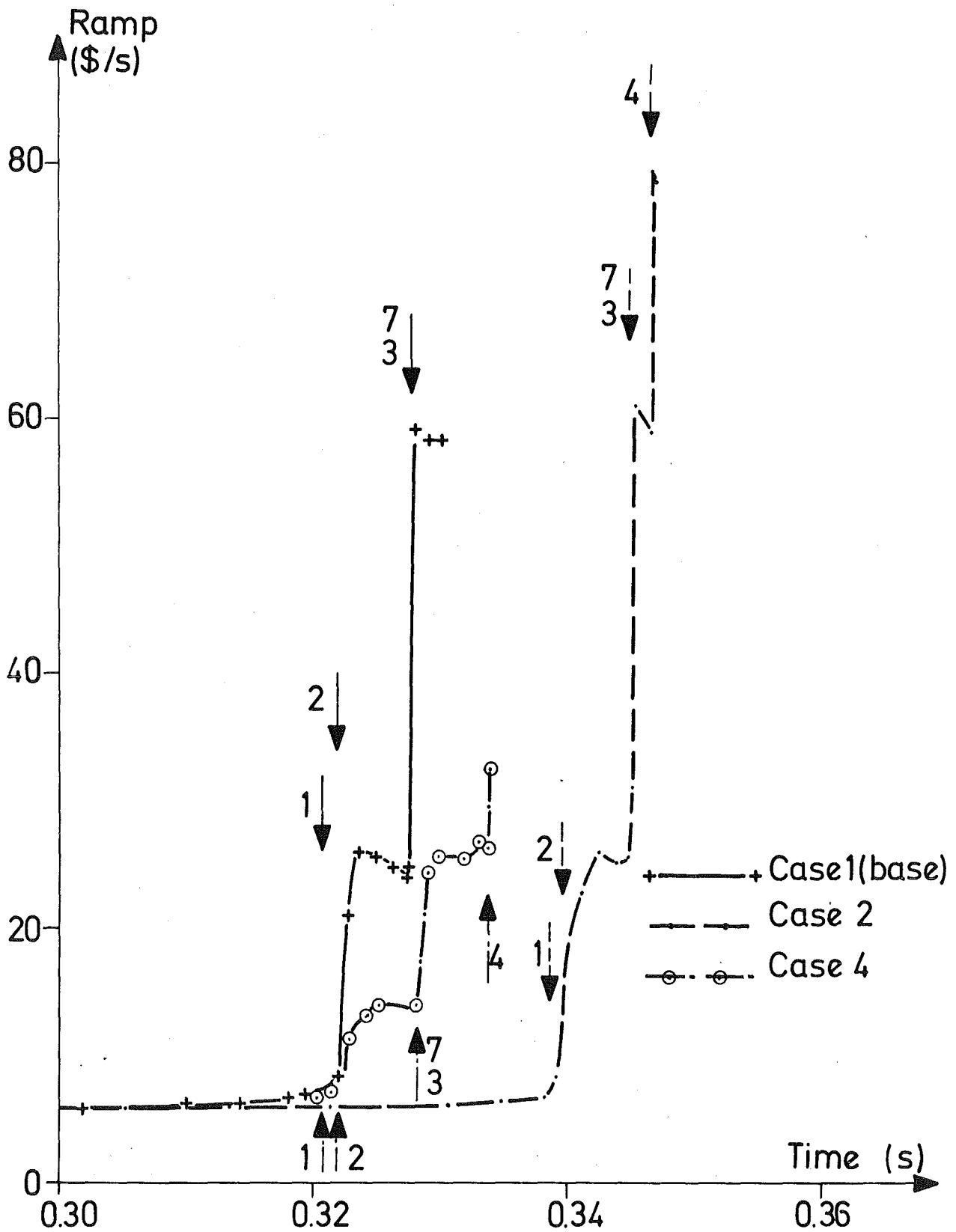
POSITIVE REACTIVITY RAMP VERSUS TIME

FIG.4
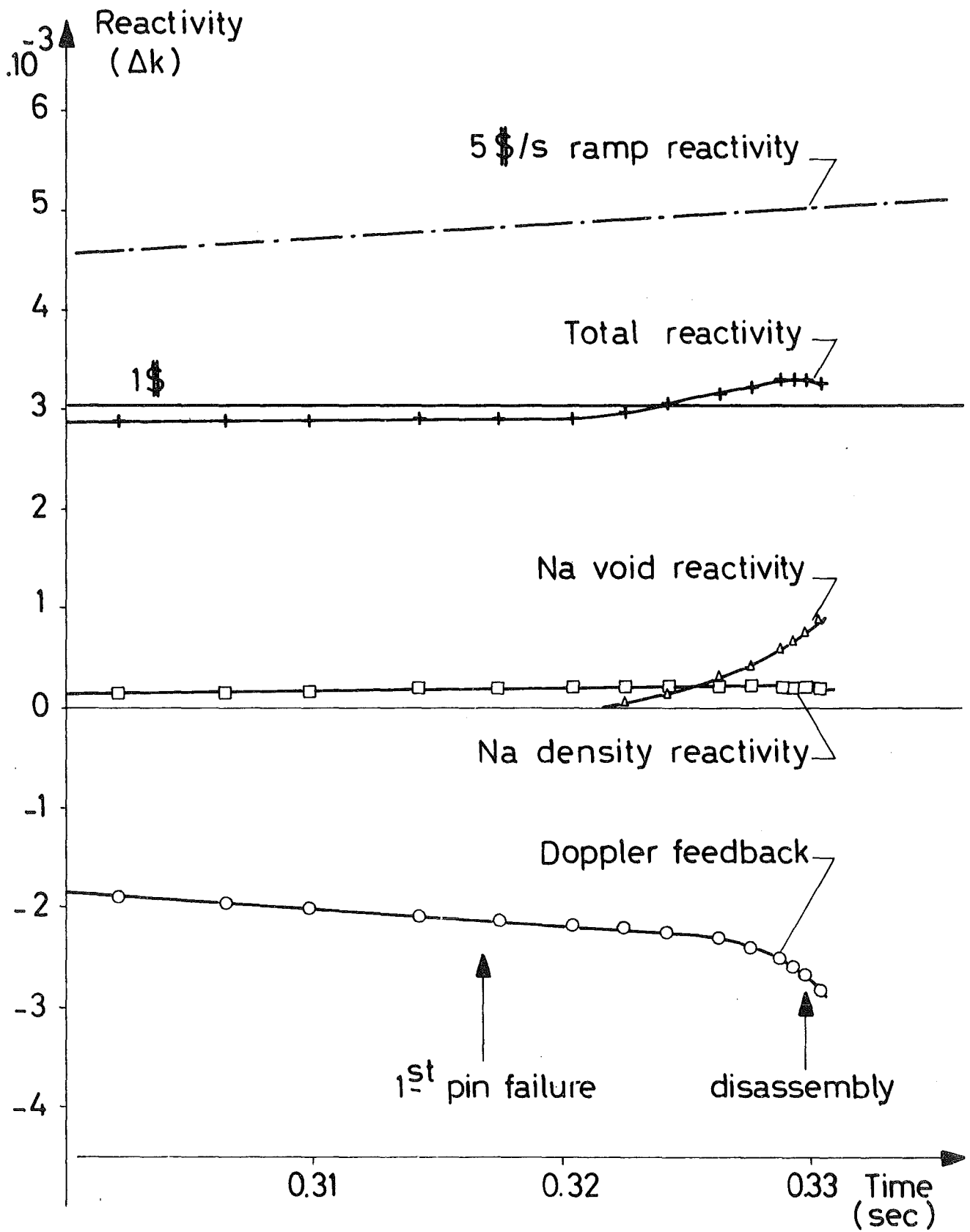
BASE CASE – REACTIVITY COMPONENTS
VERSUS TIME

FIG.5
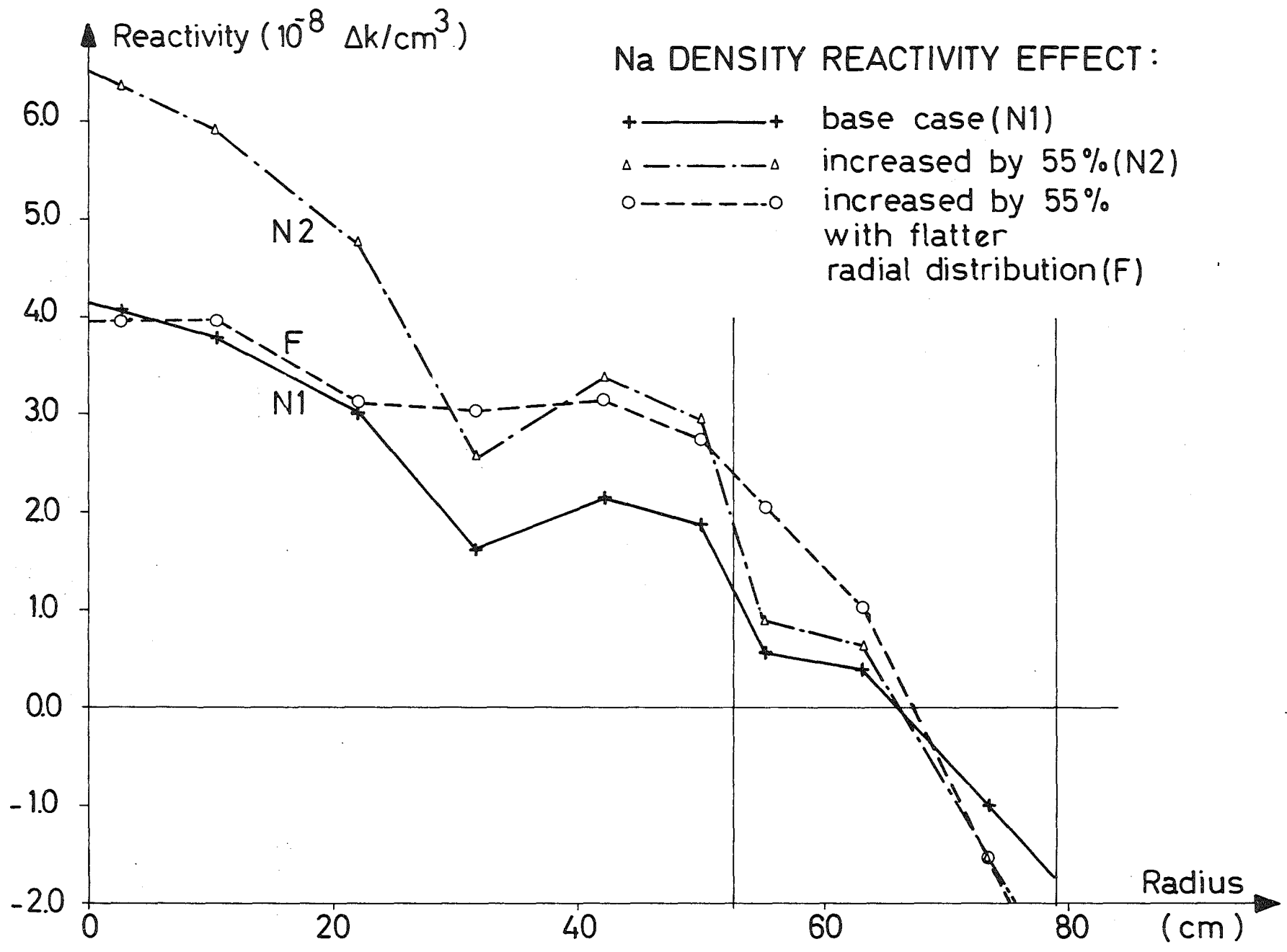
FIG.6

FIG. 7
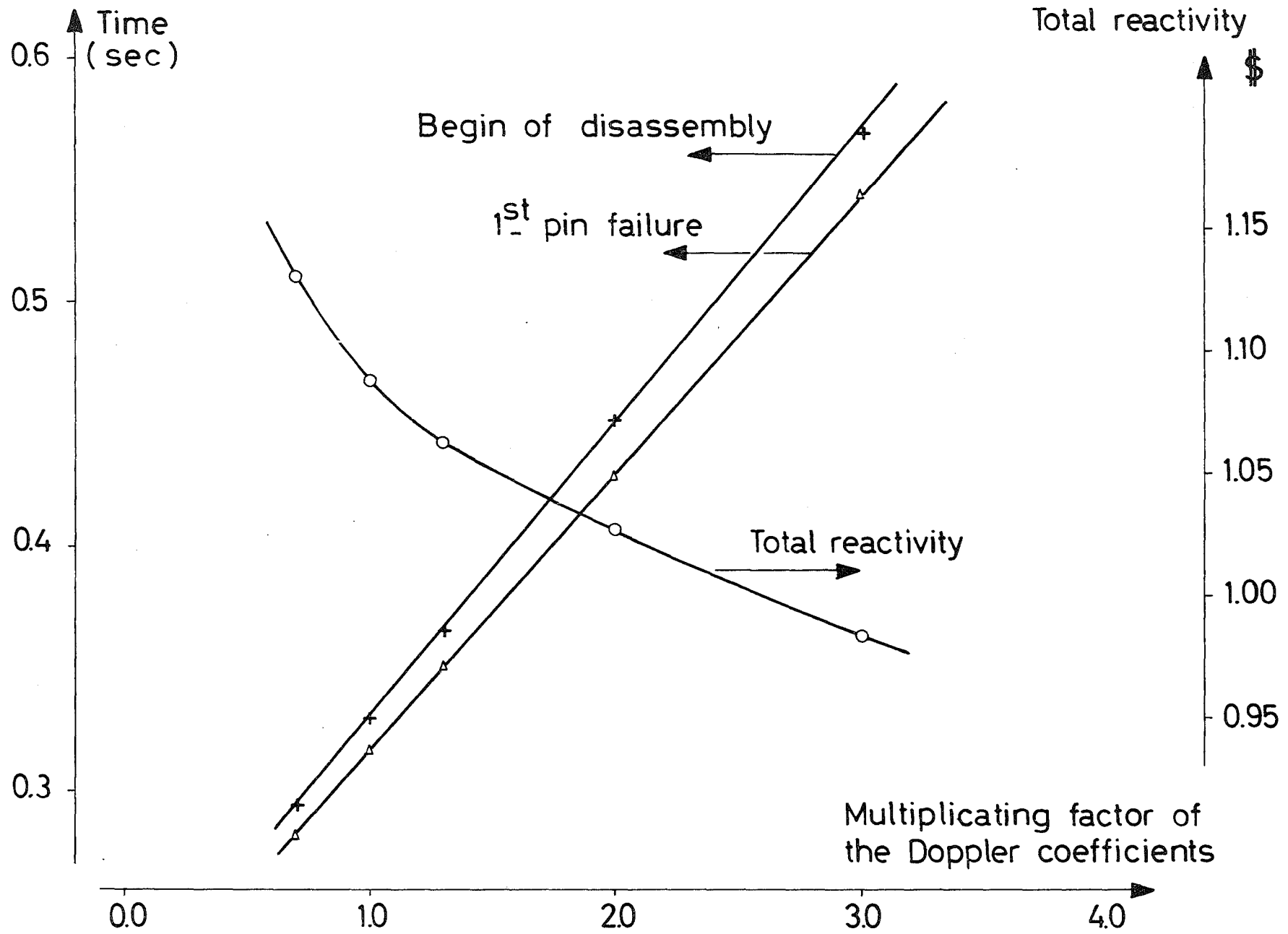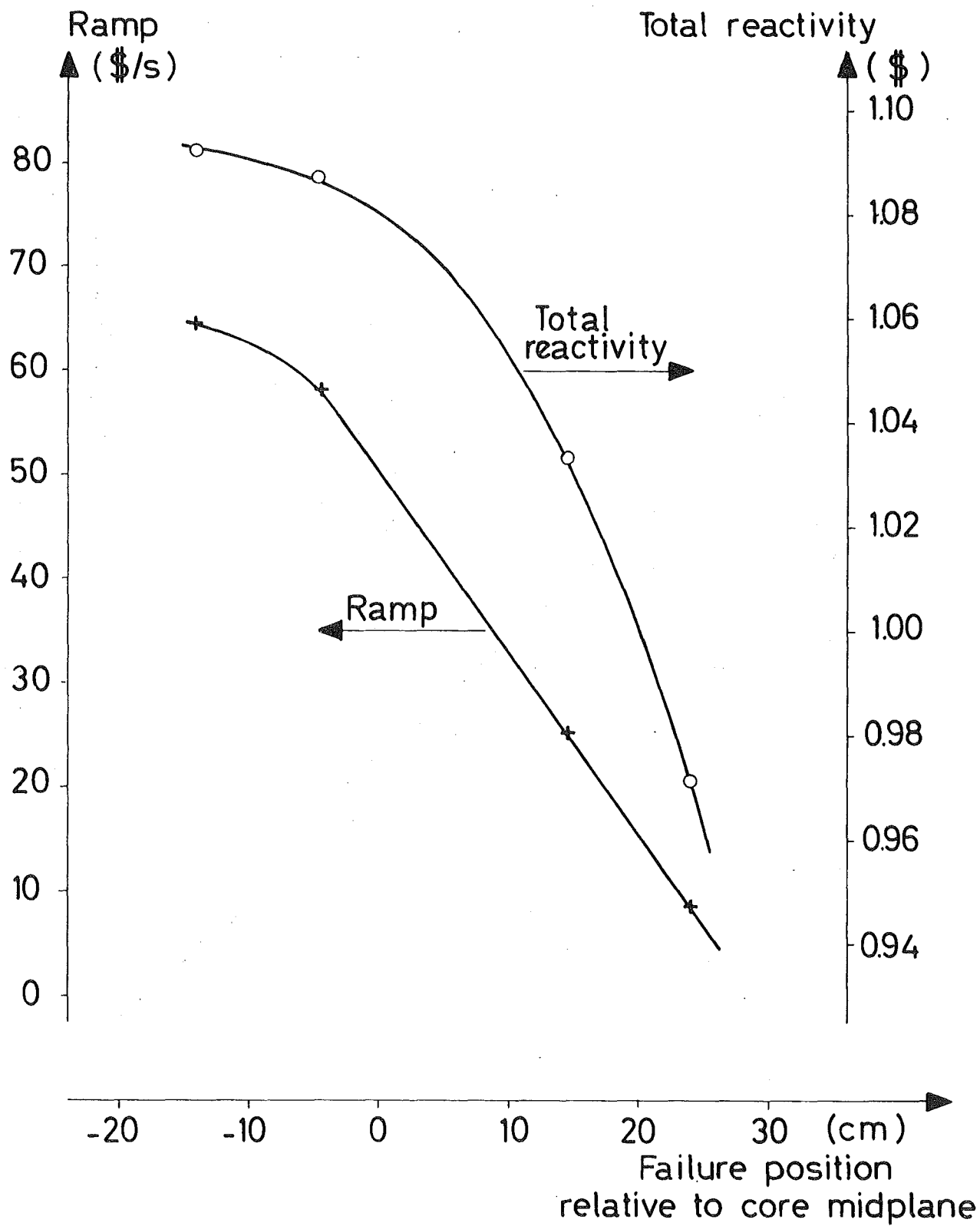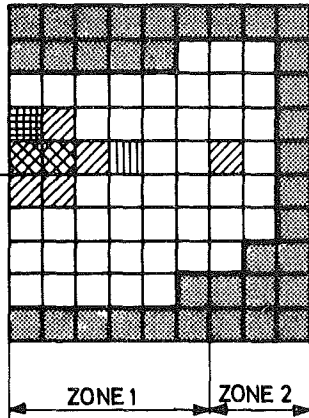
FIG.8

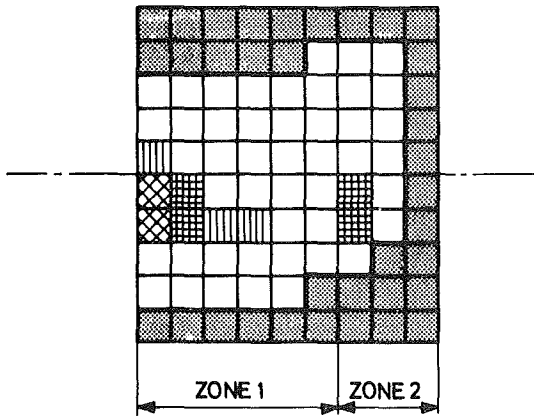# SODIUM VOIDING PATTERN AT
THE BEGINNING OF DISASSEMBLY

BASE CASE

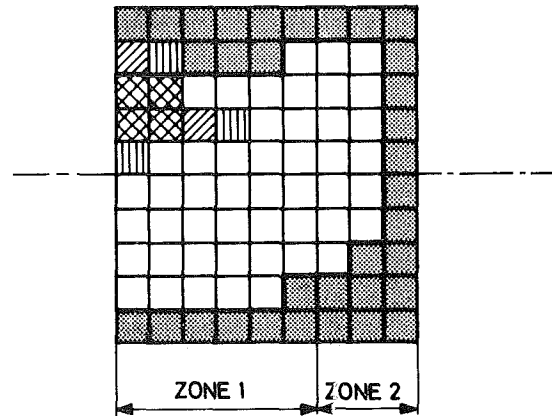05 $/s RAMP ACCIDENT

ZONE 1   ZONE 2

ZONE 1   ZONE 2
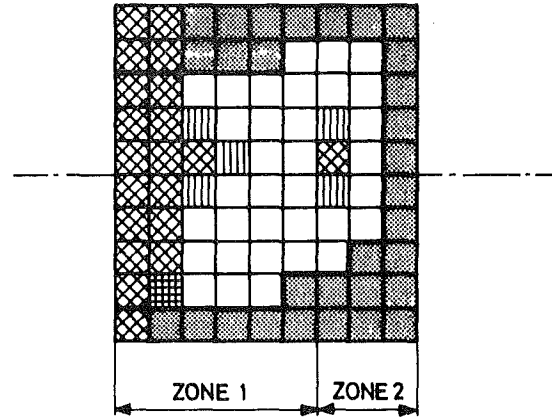
PIN FAILURE IS LOCATED
14 cm BELOW CORE MIDPLANE

PIN FAILURE IS LOCATED
14 cm ABOVE CORE MIDPLANE

ZONE 1   ZONE 2

ZONE 1   ZONE 2

LEGEND
☐ POSITIVE SODIUM VOID REACTIVITY

▨ NEGATIVE SODIUM VOID REACTIVITY

▨ Na void > 75 %

▤ Na void > 50 %

▨ Na void > 25 %

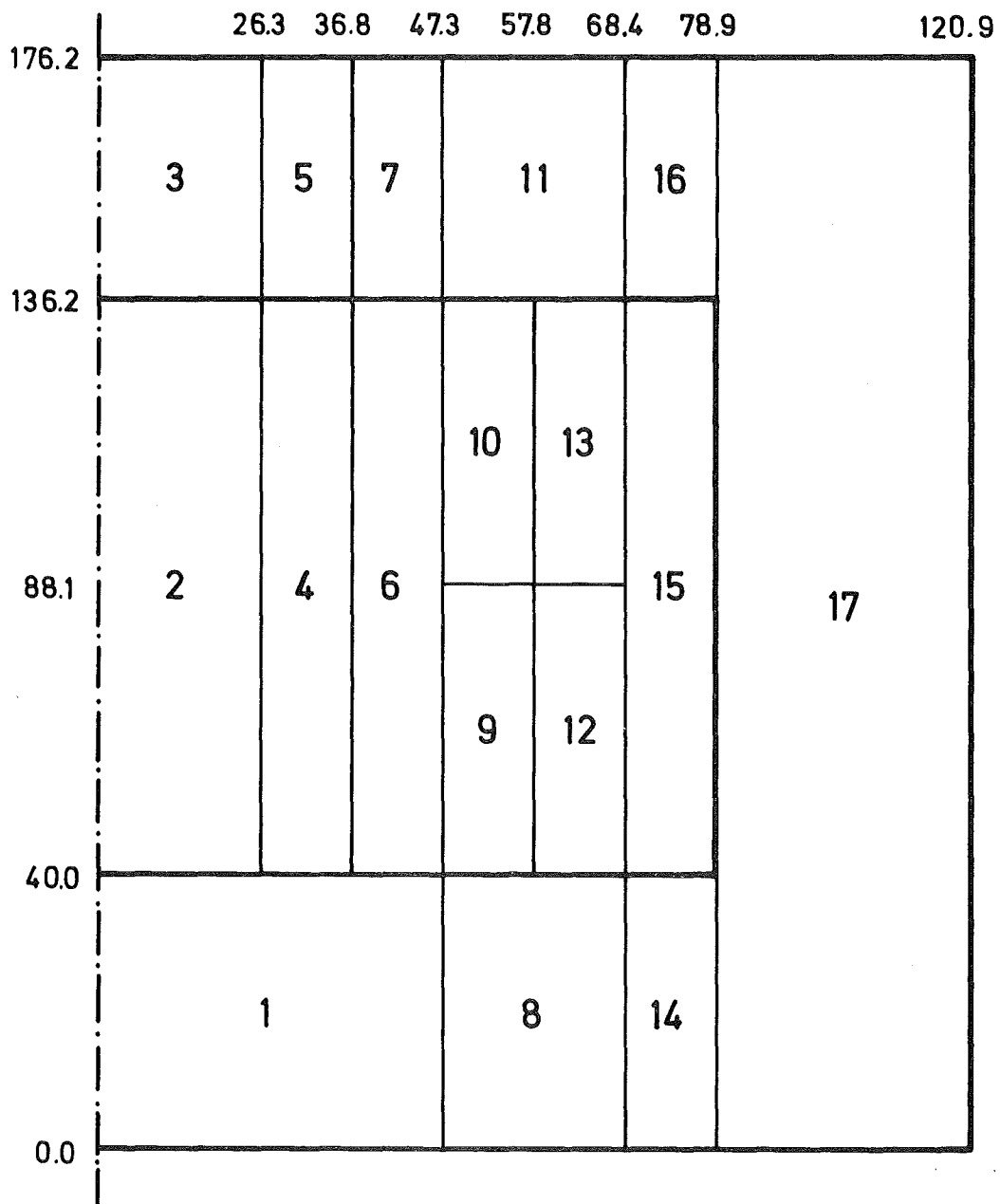▥ Na void ≥ 1 %

☐ no void

FIG.9

FIG.10: REGIONS SPECIFIED IN GEOMETRICAL MOCK-UP (KADIS)
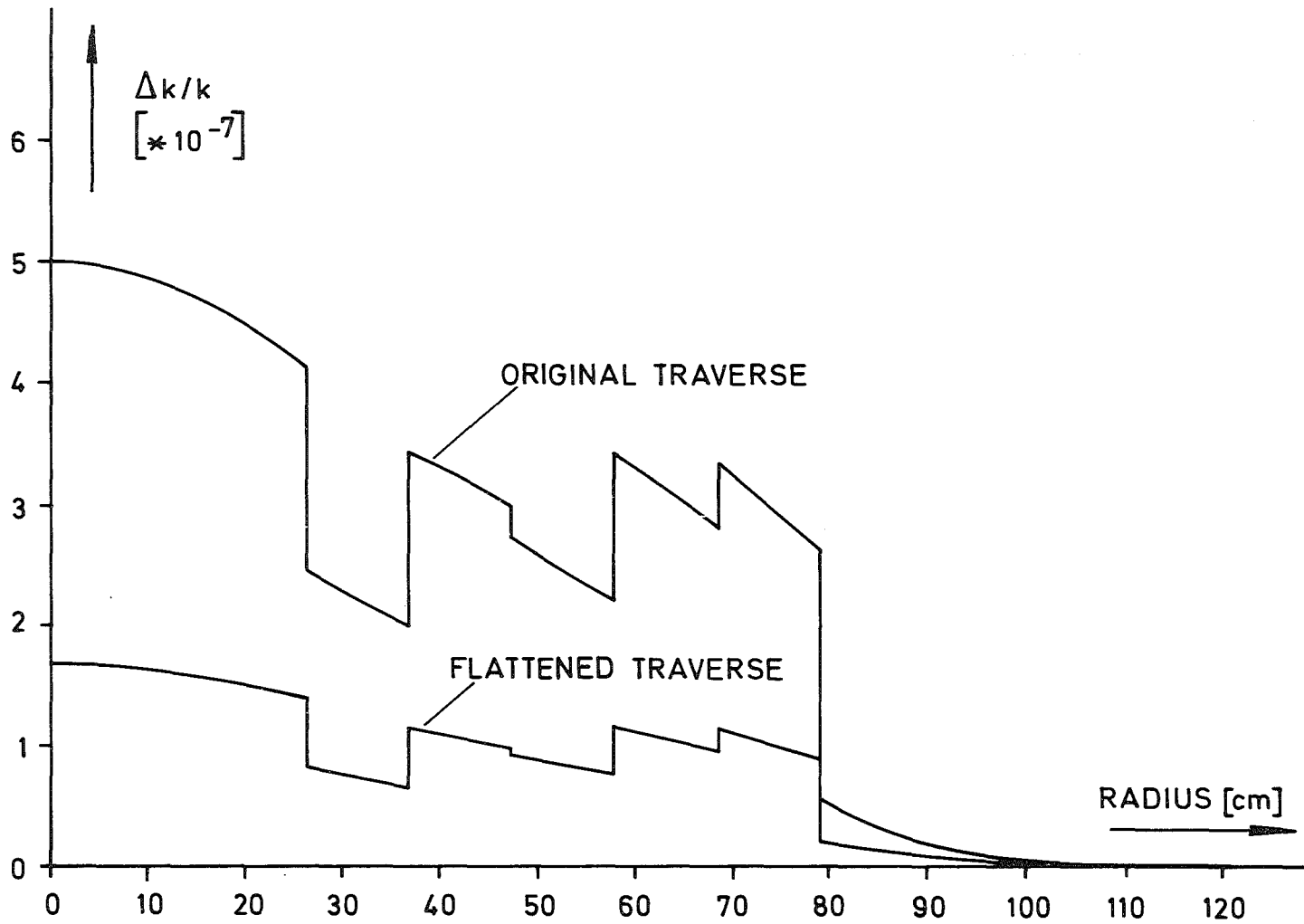
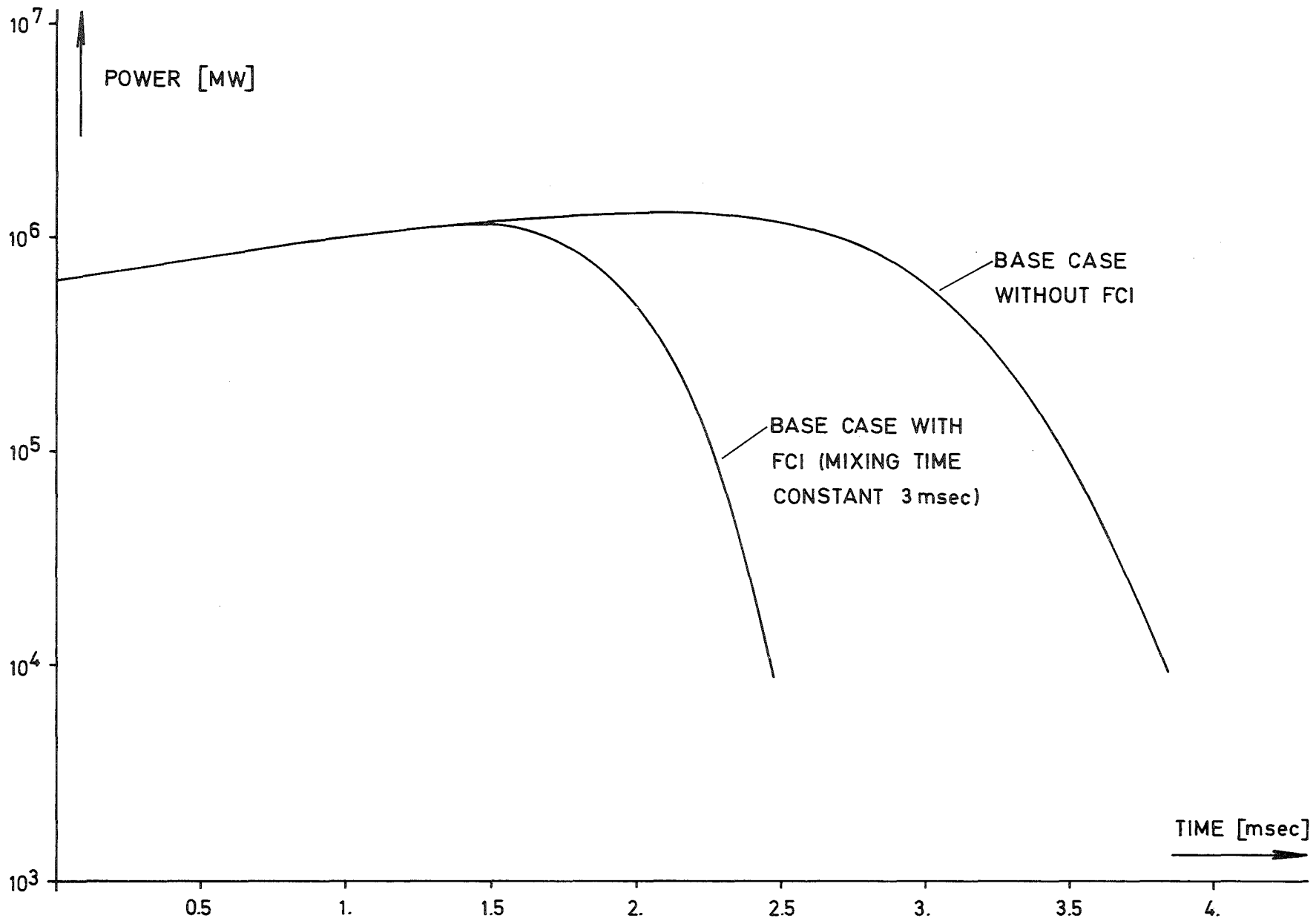FIG. 11: TOTAL MATERIAL WORTH CURVES   (RADIAL TRAVERSE BELOW MID-PLANE)

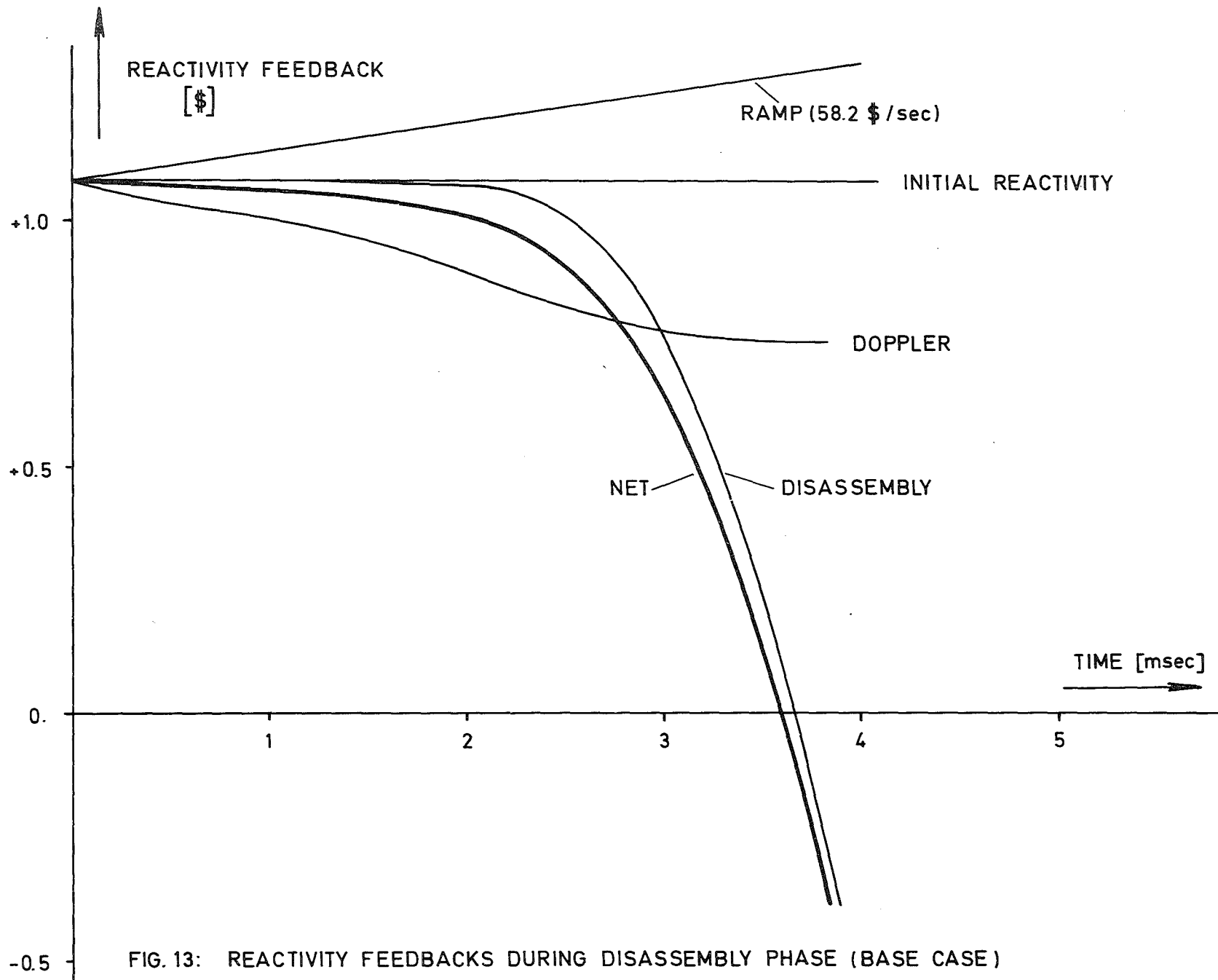FIG.12: POWER VERSUS TIME DURING DISASSEMBLY PHASE

FIG. 13: REACTIVITY FEEDBACKS DURING DISASSEMBLY PHASE (BASE CASE)
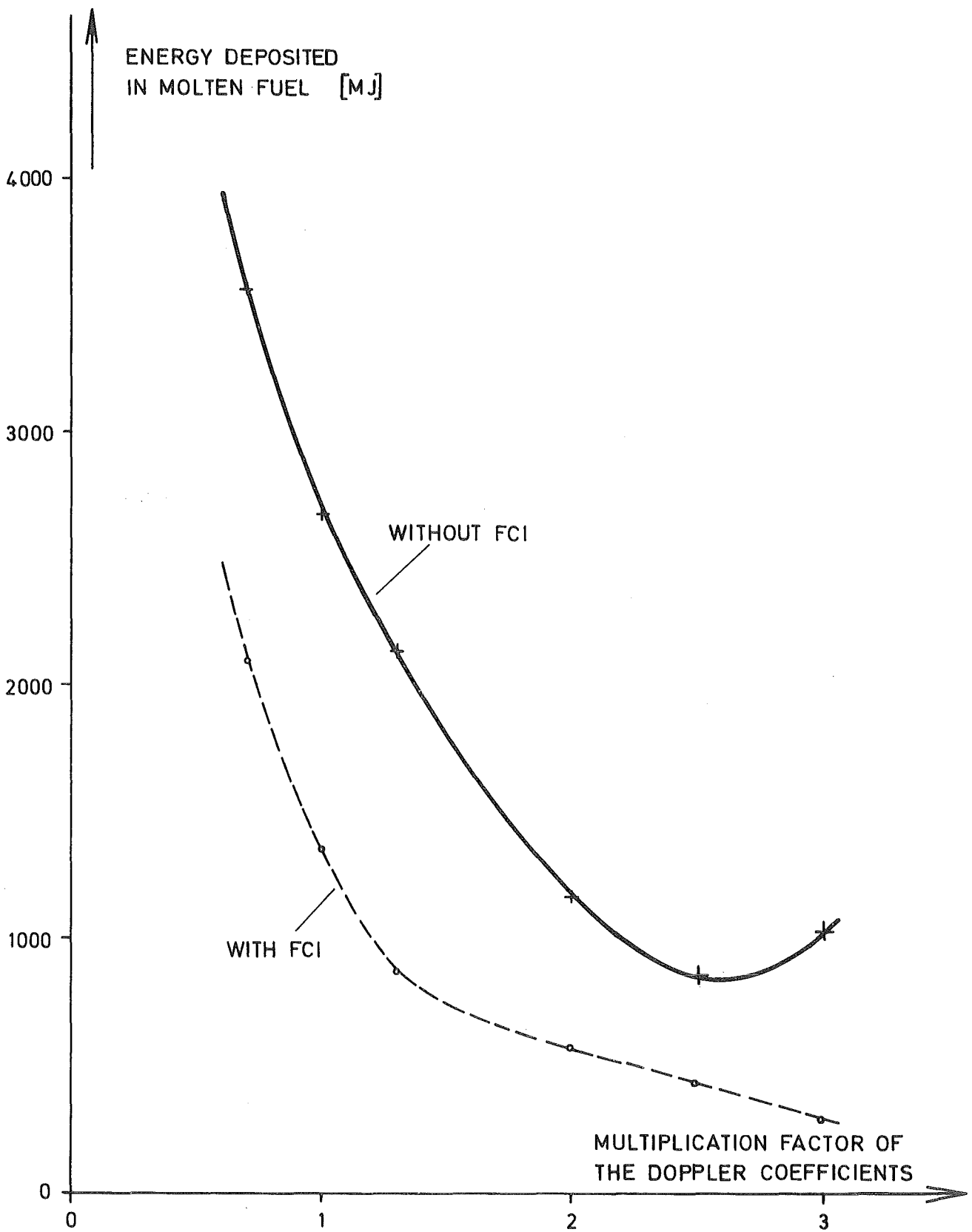
FIG.14: ENERGY OF MOLTEN FUEL VERSUS DOPPLER STRENGTH

CASE	1(BASE)	2	3	4	5
DATA					
RAMP ($/sec)	5.0	5.0	5.0	5.0	0.5
RADIAL POWER SHAPE FACTOR	1.368	1.169	1.368	1.368	1.368
AVERAGE POWER PER PIN (kW)	27.6	27.6	22.1	27.6	27.6
VOID UPPER LIMIT VELOCITY (cm/sec)	1760	1760	1760	587	1760
VOID LOWER LIMIT VELOCITY (cm/sec)	735	735	735	245	735
RESULTS					
TIME OF FIRST PIN FAILURE (sec)	0.3168	0.3347	0.3457	0.3168	2.394
TIME OF CORE DISASSEMBLY BEGIN (sec)	0.3298	0.3470	0.3583	0.3337	2.459
RAMP ($/sec)	58.20	78.43	57.20	26.02	26.74
TOTAL REACTIVITY ($)	1.087	1.106	1.095	1.028	1.050
POWER (10^6 MW)	0.635	0.851	0.734	0.313	0.540
ENERGY STORED IN THE FUEL (MJ)	3784	4613	4232	3740	3778

TABLE I   INPUT DATA AND RESULTS OF CARMEN PREDISASSEMBLY CALCULATIONS

CASE	1(BASE)	6	7	8
DATA				
RAMP ($/sec)	5.0	5.0	5.0	5.0
INCREASE OF POSITIVE Na DENSITY REACT. (%)	0.0	55	55	55
INCREASE OF POSITIVE Na VOID REACT. (%)	0.0	28	28	55
RADIAL DISTRIBUTION OF Na REACTIVITY	N1	N2	F	F
RESULTS				
TIME OF FIRST PIN FAILURE (sec)	0.3168	0.3096	0.3093	0.3093
TIME OF CORE DISASSEMBLY BEGIN (sec)	0.3298	0.3211	0.3219	0.3217
RAMP ($/sec)	58.20	79.04	80.78	96.98
TOTAL REACTIVITY ($)	1.087	1.112	1.141	1.156
POWER (10^6 MW)	0.635	0.730	0.939	0.971
ENERGY STORED IN THE FUEL (MJ)	3784	3755	3837	3816

TABLE II   INPUT DATA AND RESULTS OF CARMEN PREDISASSEMBLY CALCULATIONS

Quantity \ Problem	base case	rad. power distribution changed	power per pin 2o % lower	1/3 voiding velocity
KADIS input data				
Ramp ($/s)	58.2	78.4	57.2	26.o
Initial reactivity ($)	1.o87	1.1o6	1.o95	1.o28
Initial power (10^6 MW)	o.6356	o.85o6	o.7342	o.3125
KADIS results				
Duration (ms)	3.84	3.33	3.57	6.75
Max. power (10^6 MW)	1.31	1.75	1.39	o.361
Energy release (MJ) during the disassembly phase	326o	374o	326o	177o
Energy accumulated in the molten fuel (MJ)	2676	3811	2826	1352
Mass of molten fuel (kg)	4324	4848	4442	3o56
Average temp. of molten fuel (K)	3814	4196	3854	341o
Max. fuel temperature (K)	5823	6213	5848	4655

Table III   Results of consistent CARMEN/KADIS sensitivity calculations

Problem Quantity	base case with FCI particle radius: o.o15 cm		base case
	mixing time const: 3 ms	mixing time const: 1o ms	worth curves divided by 3
KADIS results Duration (ms)	2.48	3.6o	4.37
Max. power ($1o^6$ MW)	1.16	1.32	1.34
Energy release (MJ) during the disassembly phase	19oo	31oo	363o
Energy accumulated in the molten fuel (MJ)	1366	2464	3oo6
Mass of molten fuel (kg)	3255	4242	45o6
Average temp. of molten fuel (K)	3359	3727	3925
Max. fuel temperature (K)	45o5	5482	61o5

Table IV   Results of sensitivity studies with KADIS

Problem Quantity	s.v. + 28 % s.d. + 55 %	flatter rad. distribution	
		s.v. + 28 % s.d. + 55 %	s.v. + 55 % s.d. + 55 %
KADIS input data Ramp ($/s)	79.0	80.8	97.0
Initial reactivity ($)	1.112	1.141	1.156
Initial power (10^6 MW)	0.7295	0.9390	0.9707
KADIS results Duration (ms)	3.26	2.79	2.57
Max. power (10^6 MW)	1.93	2.35	2.86
Energy release (MJ) during the disassembly phase	3830	4010	4310
Energy accumulated in the molten fuel (MJ)	3172 (+19%)	3406 (+27%)	3639 (+36%)
Mass of molten fuel (kg)	4577	4684	4754
Average temp. of molten fuel (K)	3984	4062	4149
Max. fuel temperature (K)	6251	6422	6643

Table V   Results of CARMEN/KADIS calculations with changed sodium
reactivity coefficients. The values in parentheses indicate
the change as compared to the base case.

| Quantity \ Problem | pin failure located at | | 0.5 $/s– ramp at initiation |
	14 cm above core midplane	14 cm below core midplane	
KADIS input data			
Ramp ($/s)	25.2	64.5	26.7
Initial reactivity ($)	1.034	1.093	1.050
Initial power (10^6 MW)	0.1919	0.5582	0.5395
KADIS results			
Duration (ms)	7.59	3.80	5.12
Max. power (10^6 MW)	0.340	1.49	0.624
Energy release (MJ) during the disassembly phase	1800	3450	2070
Energy accumulated in the molten fuel (MJ)	1363 (−48%)	2811 (+5%)	1547 (−42%)
Mass of molten fuel (kg)	3064	4392	3165
Average temp. of molten fuel (K)	3416	3863	3516
Max. fuel temperature (K)	4677	5956	4909

Table VI   Results of CARMEN/KADIS calculations with changed pin failure location and lower ramp. The values in parentheses indicate the change as compared to the base case.